Insights into Imaging

ORIGINAL ARTICLE

Open Access

# Feasibility of utilizing ultra-low-dose contrast medium for pancreatic artery depiction using the combination of advanced virtual monoenergetic imaging and high-concentration contrast medium: an intra-patient study

Juan Li[1†], Yu-hong Wang[1†], Fu-ling Zheng[1†], Xin-yue Chen[2], Yun Lin[3], Cai-rong Zhu[4], Yi-fan Wu[3], Qiang Xu[5], Zheng-yu Jin[1*] and Hua-dan Xue[1*]

## Abstract

**Objectives:** The least amount of contrast medium (CM) should be used under the premise of adequate diagnosis. The purpose of this study is to evaluate the feasibility of utilizing ultra-low-dose (224 mgI/kg) CM for pancreatic artery depiction using the combination of advanced virtual monoenergetic imaging (VMI+) and high-concentration (400 mgI/mL) CM.

**Materials and methods:** 41 patients who underwent both normal dose CM (ND-CM, 320 mgI/kg) and low dose CM (LD-CM, 224 mgI/kg) thoracoabdominal enhanced CT for tumor follow-up were prospectively included. The VMI+ at the energy level of 40-kev for LD-CM images was reconstructed. CT attenuation, signal-to-noise ratios (SNRs), and contrast-to-noise ratios (CNRs) of the abdominal artery, celiac artery, and superior mesenteric artery (SMA) and qualitative scores of pancreatic arteries depiction were recorded and compared among the three groups (ND-CM, LD-CM, and VMI+ LD-CM images). ANOVA and Friedman tests were used for statistical analysis.

**Results:** All quantitative and qualitative parameters on LD-CM images were lower than that on ND-CM images (all $p < 0.01$). There were no significant differences of all arteries' qualitative scores between ND-CM and VMI+ LD-CM images (all $p > 0.05$). VMI+ LD-CM images had the highest mean CT and CNR values of all arteries (all $p < 0.0001$). The CM volume was $52.6 \pm 9.4$ mL for the ND-CM group and $37.0 \pm 6.7$ mL for the LD-CM group.

**Conclusion:** Ultra-low-dose CM (224 mgI/kg) was feasible for depicting pancreatic arteries. Inferior angiographic image quality could be successfully compensated by VMI+ and high-concentration CM.

*Correspondence: jinzy@pumch.cn; bjdanna95@hotmail.com
†Juan Li, Yu-hong Wang and Fu-ling Zheng have contributed equally to this work
[1] Department of Radiology, State Key Laboratory of Complex Severe and Rare Disease, Peking Union Medical College Hospital, Chinese Academy of Medical Sciences, Peking Union Medical College, Beijing, China
Full list of author information is available at the end of the article

**Keywords:** Computed tomography angiography, Pancreas, Arteries, Contrast media

## Key Points

- Ultra-low dose (224 mgI/kg) contrast medium could be used for pancreatic artery depiction.
- Reduced image quality could be compensated by VMI+ technique.
- This imaging strategy can save half of contrast medium costs.

## Background

Abdominal CTA is widely used to assess vascular disorders [1] and guide surgical planning for patients with tumors [2]. However, the contrast medium (CM) dosage is associated with contrast-induced nephropathy and other chemotoxic reactions [3, 4]. The European Society of Urogenital Radiology guidelines recommend that the least amount of CM should be used under the premise of adequate diagnosis [5]. Nevertheless, sufficient CM is necessary for the depiction of small vessels [6]. Pancreas is a hypervascular organ, and the average diameter of the lumen of pancreatic arteries of approximately 2 mm [7]. Although the resectability of pancreatic carcinoma depends on the main vessels around the pancreas, pancreatic arteries have been reported to correlate with blood loss in surgeries, which is a known risk factor for postoperative complications [8]. For instance, for pancreaticoduodenectomy using the artery as the first approach, the preoperative identification of inferior pancreaticoduodenal artery (IPDA) on CT angiography allows IDPA ligation in a shorter time. Moreover, the successful ligation of IDPA before an efferent vein resolves the main cause of intraoperative blood loss in pancreaticoduodenectomy. In addition, for more dedicated surgeries such as pancreas transplants, understanding the different pancreatic artery types is important to prevent possible complications [9]. Therefore, using techniques for good pancreatic arteries visualization that allows the least amount of CM is of great importance.

Methods for improving abdominal CTA image quality acquired using a reduced dose of CM include virtual monochromatic imaging (VMI) [6], test-bolus injection [10], low-tube-voltage imaging [11, 12], CTA individual-delay bolus tracking [13], multiphasic injection [14] and high-concentration CM imaging [15]. Notably, the abovementioned methods are widely used for CM dose reduction in the imaging of the abdominal aorta and its main branches. Only a few studies have focused on small arteries. According to Sugawara H et al. [6], though half-iodine dose (300 mgI/kg) VMI could depict large vessels comparable to full-iodine dose (600 mgI/kg) conventional CT, VMI failed to visualize small arteries clearly. The concentration of CM in their study was 300 mgI/mL. On the contrary, in another study, Holalkere NS et al. [15] used high-concentration CM (370 mgI/mL) and demonstrated that the third to the fifth order branches of the superior mesenteric artery (SMA) could be depicted clearly with 20% less iodine dose (full-iodine dose: 600 mgI/kg, 20% less-iodine dose: 480 mgI/kg).

As for a fixed volume of CM and a constant injection rate, a higher concentration of CM could produce a greater magnitude of aortic enhancement by increasing the iodine delivery rate (IDR). Moreover, with the advanced virtual monoenergetic imaging (VMI+) technique, images reconstructed at the energy level of 40 keV, which is the closest possible to the K-edge of iodine (33 keV), have better quality than images reconstructed using the VMI technique [16]. In this study, we hypothesized that by combining high-concentration CM (400 mgI/mL) and VMI+, ultra-low-dose CM (224 mgI/kg) abdominal CTA images could depict both large vessels and pancreatic arteries clearly.

The purpose of this study was to evaluate the feasibility of ultra-low-dose CM (224 mgI/kg) for depicting abdominal arteries, especially for pancreatic artery visualization, using the combination of VMI+ and high-concentration CM (400 mgI/mL).

## Materials and methods

This prospective study was approved by the Institutional Review Board of Peking Union Medical College Hospital. Written informed consent was obtained from all patients.

### Subjects

From April 2019 to May 2020, 124 consecutive patients who received follow-up thoracoabdominal enhanced CT scans at our hospital for post-treatment tumor surveillance were enrolled in this study. The exclusion criteria were as follows: (1) patients with contraindications to intravenous administration of iodine CM; (2) patients with pancreatic mass, with consideration that it might affect pancreatic arteries depiction; (3) structural changes of abdominal blood vessels caused by surgery; (4) patients whose follow-up CTs were lost in our hospital. Finally, 41 patients were included in this study after excluding 3 patients with structural changes in the abdominal blood vessels caused

by surgery (2 patients underwent total gastrectomy and 1 patient underwent splenectomy), 2 patients with pancreatic mass, and 78 patients with lost follow-up CT.

### Study design

This was an intra-patient study in which each patient consecutively received both normal-dose CM (ND-CM, 400 mgI/mL, 0.8 mL/kg, and 320 mgI/kg) and low-dose CM (LD-CM, 400 mgI/mL, 0.56 mL/kg, and 224 mgI/kg) in a random order for the first scan and follow-up to minimize patient factors that would affect artery visualization. High-concentration CM was used in our study to achieve high IDR under a constant injection rate. The CM concentration and injection rate, which determine the IDR, were the same in the two groups such that the CM dose would be the only factor affecting the magnitude of artery enhancement. The rationale for the low-dose group design was that we assumed that a 30% reduction of the normal-dose group was feasible, as previous low-dose studies of low kVp [17] or dual-energy [18, 19] enabled a 50% reduction of iodine load at most.

### CT examination

All patients underwent thoracoabdominal enhanced CT using a 192-detector MDCT scanner (Siemens Somatom Force; Siemens, Forchheim, Germany). The CM was warmed to achieve normal body temperature (37 °C) before injection. After performing topogram and nonenhanced scan, patients received the CM at a rate of 4 mL/s, followed by 40 mL of saline at the same rate. Using bolus tracking, the arterial phase was initiated for 5 s for the LD-CM group and 6 s for the ND-CM group after achieving the threshold density of 100 HU in the aortic arch. The scanning parameters were as follows: 100 kV/250 (ref. mAs for tube A); 150 kV/125 (ref. mAs for tube B); pitch, 1.2; collimation, 128 × 0.6 mm; rotation time, 0.5 s; kernel Br40f, 0.6 mm slice thickness and 0.4 mm slice increment were used for vascular evaluation.

### Image post-processing

Arterial phase images were transferred to a workstation (syngo.via, version VB10, Siemens Healthineers) for analysis. VMI+ images at the energy level of 40 keV of the LD-CM scanning were reconstructed. The coronal maximum intensity projection (MIP) images (10-mm thickness, 1-mm interval) of the ND-CM scanning, LD-CM scanning, and VMI+ images of the LD-CM scanning were reconstructed for analysis.

### Image assessment

#### *Quantitative analysis of abdominal aorta and its main branches*

Circular regions of interest (ROIs) were drawn by one radiologist on the abdominal aorta at the level between the celiac artery orifice and the SMA, the celiac artery, SMA and right erector spinae muscle on axial images (Fig. 1) of the ND-CM scanning, LD-CM scanning, and VMI+ images of the LD-CM scanning using an independent DICOM viewer (Medixant. RadiAnt DICOM Viewer. Version 4.6.9. Oct 25, 2018. URL: https://www.radiantviewer.com). The ROIs were carefully drawn to avoid the wall, the calcification or noncalcified plaque of the vessels, and artifacts. The size and shape of the ROIs were kept constant using the copy-and-paste function. The average and standard deviation (SD) values of CT attenuation of all ROIs were recorded. The SD of the right erector spinae muscle was used to define the image noise. Signal-to-noise ratios (SNRs) of vessels were calculated by $\text{Mean}_{\text{vessel}}(\text{HU})/\text{SD}_{\text{vessel}}(\text{HU})$. Contrast-to-noise ratios (CNRs) of vessels were calculated as follows: $(\text{Mean}_{\text{vessel}}(\text{HU}) - \text{Mean}_{\text{muscle}}(\text{HU}))/\text{SD}_{\text{muscle}}(\text{HU})$.

#### *Qualitative analysis of abdominal aorta, its main branches, and pancreatic arteries*

The axial and coronal multiplanar reformation images (thickness: 0.6 mm) and coronal MIP images of ND-CM scanning, LD-CM scanning, and VMI+ images of LD-CM scanning were read by two radiologists (one with 4 years of experience and the other with more than 10 years of experience in abdominal imaging) using the same DICOM viewer. The readers were blinded to the clinical information or identification of the reconstruction method. The three groups of images from each patient were randomized, and the readers evaluated one set at a time in a random order, with a time interval of 2 weeks. The visualization of the abdominal artery, celiac artery, and SMA were graded using a 4-point scale: 1 = no depiction, 2 = faint depiction, 3 = good depiction, and 4 = excellent depiction. Pancreatic arteries (posterior superior pancreaticoduodenal artery [PSPDA]; anterior superior pancreaticoduodenal artery [ASPDA]; inferior pancreaticoduodenal artery [IPDA]; anterior inferior pancreaticoduodenal artery [AIPDA]; posterior inferior pancreaticoduodenal artery [PIPDA]; dorsal pancreatic artery [DPA]; transverse pancreatic artery [TPA]; great pancreatic artery [GPA]; and caudal pancreatic artery [CPA]) were graded using a 4-point scale: 0 = not visible, 1 = partially visible, 2 = partially invisible or slightly irregular appearance, and 3 = completely visible [6]. First, a qualitative scoring of pancreatic arteries was performed on the coronal MIP images. If considered invisible, the axial and coronal images were then used to confirm that the pancreatic arteries were invisible. Any inconsistent results were discussed by the two radiologists to make a final decision. The luminal diameters of pancreatic arteries were then measured using multiplanar reconstruction following curvilinear planes [7, 20]. The depiction rate of

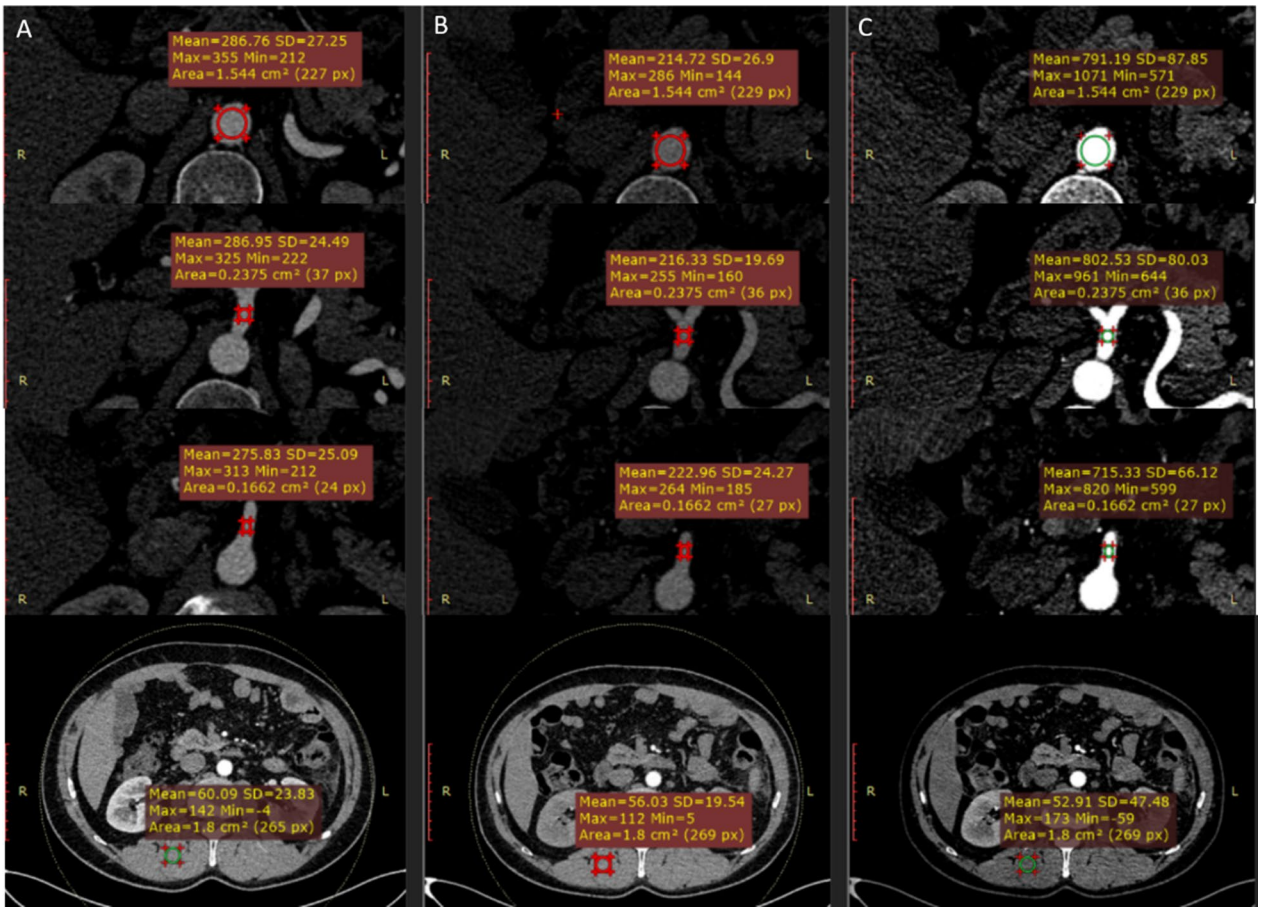


**Fig. 1** Quantitative analysis of main branches of abdominal arteries. **a**–**c** ND-CM (0.8 mL/kg, 400 mgI/mL, and 320 mgI/kg), LD-CM (0.56 mL/kg, 400 mgI/mL, and 224 mgI/kg), and VMI+ LD-CM images in the same patient. Images show the ROI for attenuation measurement at the level of the aorta (first line), celiac artery (second line), superior mesenteric artery (SMA, third line), and right erector spinae muscle (last line). *ND-CM* normal-dose contrast medium, *LD-CM* low-dose contrast medium, *VMI+* advanced virtual monoenergetic imaging

pancreatic arteries was calculated by dividing the number of patients with visible pancreatic arteries by the total number of patients.

### Statistical analysis

All statistical analyses were performed using SAS software version 9.4 (SAS Institute, Inc., Cary, NC, USA). Continuous variables with normal distribution were expressed as mean ± SD. Categorical and continuous variables without normal distribution were displayed in median (quartile 2, quartile 3). The paired t-test or Wilcoxon test was used to compare the differences in patient demographics and contrast dose parameters between ND-CM and LD-CM groups. When comparing the differences in parameters among the three groups, if continuous variables satisfied both normal distribution and homogeneity of variance, a randomized block ANOVA was used to compare intergroup differences; otherwise, the Friedman test was used. The differences of qualitative scores among the three groups were compared using the Friedman test. A $p$ value < 0.05 were considered statistically significant. Interobserver agreement for qualitative evaluation was assessed by Cohen's kappa ($\kappa$) analysis: $\kappa$ of < 0 indicative poor agreement, 0–0.20 slight agreement, 0.21–0.40 fair agreement, 0.41–0.60 moderate agreement, 0.61–0.80 substantial agreement, and 0.81–1 almost perfect agreement.

## Results

### Patient population

A total of 41 patients including 26 males and 15 females (mean age, 56 ± 13 years; age range, 24–77 years) were included in this study. Primary diseases among the patients were colorectal cancer ($n = 14$), lung cancer ($n = 10$), esophageal cancer ($n = 3$), gastric cancer ($n = 2$), thymic carcinoma ($n = 2$), breast cancer ($n = 1$), peritoneal mesothelioma ($n = 1$), testicular cancer ($n = 1$), stromal sarcoma ($n = 1$), leiomyosarcoma

($n=1$), hypopharyngeal carcinoma ($n=1$), angioendothelioma ($n=1$), rectal stromal tumor ($n=1$), appendix mucinous adenocarcinoma ($n=1$), and soft tissue sarcoma ($n=1$). The interval between the first examination and the follow-up was $135\pm78$ days. The data on patient demographics and contrast dose are listed in Table 1.

**Table 1** Patient demographics ($n=41$) and contrast dose

| Variables | ND-CM | LD-CM | *p* value |
|---|---|---|---|
| Age (y) | 56.1 ± 13.1 | 56.0 ± 13.0 | 0.1250 |
| Sex | | | |
| Male | 26 | 26 | – |
| Female | 15 | 15 | – |
| Weight (kg) | 65.74 ± 11.81 | 66.00 ± 11.99 | 0.7614 |
| Height (cm) | 165.59 ± 8.74 | 165.59 ± 8.58 | 1.0000 |
| Body mass index (kg/cm$^2$) | 24.07 ± 3.59 | 24.08 ± 3.63 | 0.3009 |
| Iodine dose (mgI/kg) | 320 | 224 | – |
| Iodine volume | 52.59 ± 9.44 | 36.96 ± 6.71 | < 0.0001 |
| Capacity per bottle (mL) | 50 | 50 | – |

Data are means ± standard deviations

The difference between ND-CM group and LD-CM group by using the paired t test or Wilcoxon signed test. $p<0.05$ is considered statistically significant

ND-CM: normal dose contrast medium (320 mgI/kg), LD-CM: low dose contrast medium (224 mgI/kg)

### Quantitative analysis of abdominal aorta and its main branches

Mean CT and CNR values of all vessels were the highest in VMI+ LD-CM images, followed by ND-CM images, and the lowest in LD-CM images (all $p<0.0001$). The SNR values of all vessels on VMI+ LD-CM and ND-CM images were higher than those in LD-CM images (all $p<0.05$). The SNR of the aorta in VMI+ LD-CM images were lower than those in ND-CM images ($p=0.0465$), whereas there was no significant difference in the SNRs of the celiac artery and SMA between ND-CM and VMI+ LD-CM images ($p=0.6911$ and 1.0000, respectively). The image noise in VMI+ LD-CM images was significantly higher than that of ND-CM and LD-CM images (both $p<0.0001$) (Table 2).

### Qualitative analysis of abdominal aorta, its main branches and pancreatic arteries

There was substantial to perfect agreement between the two readers in qualitative analysis of the depiction of all arteries (mean $\kappa=0.8465$, range, 0.6997–1.0000).

### Depiction rate and lumen diameter of pancreatic arteries

The depiction rates of all pancreatic arteries were higher in ND-CM images than in LD-CM and VMI+ LD-CM images (Table 3). Moreover, ND-CM images could depict all arteries visualized on LD-CM and VMI+ LD-CM images.

**Table 2** Results of quantitative analysis

| Parameters | ND-CM images* | LD-CM images* | LD-CM VMI+ images* | $p_1$ value† | $p_2$ value† | $p_3$ value† |
|---|---|---|---|---|---|---|
| *Average value (HU)* | | | | | | |
| Aorta | 337.8 ± 55.36 | 260.16 ± 73.08 | 1029.76 (735.08 ,1223.75) | < 0.0001 | < 0.0001 | < 0.0001 |
| Celiac artery | 343.42 ± 56.01 | 285.32 (213.88, 325.31) | 1078.28 (817.35, 1219.92) | < 0.0001 | < 0.0001 | < 0.0001 |
| SMA | 346.65 ± 60.24 | 285.27 (211.30, 336.15) | 1034.77 (713.07, 1227.04) | < 0.0001 | < 0.0001 | < 0.0001 |
| Right Erector spinae muscles | 53.76 ± 6.26 | 53.68 ± 4.98 | 66.79 ± 10.60 | 0.3471 | < 0.0001 | < 0.0001 |
| *Image noise (HU)* | | | | | | |
| Right Erector spinae muscles | 19.99 ± 3.67 | 19.79 ± 3.33 | 44.15 ± 9.41 | 0.5136 | < 0.0001 | < 0.0001 |
| *Signal to noise ratio (SNR)* | | | | | | |
| Aorta | 13.38 ± 2.92 | 10.38 ± 2.64 | 12.06 ± 3.29 | < 0.0001** | 0.0465** | 0.0113** |
| Celiac artery | 15.27 ± 4.10 | 11.94 ± 3.64 | 13.67 (10.27, 15.27) | < 0.0001 | 0.6911 | < 0.0001 |
| SMA | 15.1 ± 3.45 | 11.58 ± 3.55 | 14.25 ± 5.09 | < 0.0001 | 1.0000 | < 0.0001 |
| *Contrast to noise ratio (CNR)* | | | | | | |
| Aorta | 14.57 ± 3.64 | 10.46 ± 3.81 | 20.71 ± 7.30 | < 0.0001 | < 0.0001 | < 0.0001 |
| Celiac artery | 14.86 ± 3.71 | 10.85 ± 4.00 | 21.23 ± 7.17 | < 0.0001 | < 0.0001 | < 0.0001 |
| SMA | 15.03 ± 3.94 | 10.86 ± 4.06 | 21.00 ± 7.30 | < 0.0001 | < 0.0001 | < 0.0001 |

Data are means ± standard deviations or Median (P25, P75)

*ND-CM: normal dose contrast medium (320 mgI/kg), LD-CM: low dose contrast medium (224 mgI/kg), VMI+ LD-CM images: advanced virtual monoenergetic imaging of LD-CM images

***p* value was calculated by *R*

† $P_1$: the difference between ND-CM images and LD-CM images; $P_2$: the difference between ND-CM images and VMI+ LD-CM images; $P_3$: the difference between LD-CM images and VMI+ LD-CM images by using the randomized block ANOVA analysis or Friedman test. $p<0.05$ is considered statistically significant

**Table 3** Depiction rates and lumen diameters of pancreatic arteries

| Artery | lumen diameter(mm) | Depiction rates | | |
|---|---|---|---|---|
| | | ND-CM images[§] | LD-CM images[§] | LD-CM VMI+ images[§] |
| PSPDA* | 1.6 (1.5, 1.8) | 100.00% (41/41) | 95.12% (39/41) | 97.56% (40/41) |
| ASPDA* | 1.7 ± 0.3 | 100.00% (41/41) | 90.24% (37/41) | 92.68% (38/41) |
| IPDA* | 1.9 ± 0.4 | 60.98% (25/41) | 51.22% (21/41) | 51.22% (21/41) |
| AIPDA* | 1.4 ± 0.3 | 80.49% (33/41) | 73.17% (30/41) | 73.17% (30/41) |
| PIPDA* | 1.3 ± 0.3 | 87.80% (36/41) | 80.49% (33/41) | 80.49% (33/41) |
| DPA* | 1.7 ± 0.4 | 87.80% (36/41) | 78.05% (32/41) | 78.05% (32/41) |
| TPA* | 1.5 ± 0.3 | 82.93% (34/41) | 70.73% (29/41) | 70.73% (29/41) |
| GPA* | 1.5 (1.3, 1.8) | 97.56% (40/41) | 85.37% (35/41) | 85.37% (35/41) |
| CPA* | 1.3 (1.2, 1.4) | 65.85% (27/41) | 56.10% (23/41) | 56.10% (23/41) |

**PSPDA* posterior superior pancreaticoduodenal artery, *ASPDA* anterior superior pancreaticoduodenal artery, *IPDA* inferior pancreaticoduodenal artery, *AIPDA* anterior inferior pancreaticoduodenal artery, *PIPDA* posterior inferior pancreaticoduodenal artery, *DPA* dorsal pancreatic artery, *TPA* transverse pancreatic artery, *GPA* great pancreatic artery, *CPA* caudal pancreatic artery

[§] *ND-CM* normal dose contrast medium (320 mgI/kg), *LD-CM* low dose contrast medium (224 mgI/kg), *VMI+ LD-CM images* advanced virtual monoenergetic imaging of LD-CM images

The depiction rate of pancreatic arteries was calculated by dividing the number of patients with visible pancreatic arteries by the total number of patients

### Qualitative scores of the abdominal aorta, its main branches and pancreatic arteries

Qualitative scores of all arteries on VMI+ LD-CM and ND-CM images were higher than those on LD-CM images (all $p < 0.05$), except for the qualitative scores of IPDA and DPA between the VMI+ LD-CM and LD-CM images ($p = 0.2059$ and 0.1038 respectively). There were no significant differences in all arteries between the ND-CM and VMI+ LD-CM images (all $p > 0.05$) (Table 4; Figs. 2, 3).

**Table 4** Results of qualitative analysis of abdominal aorta, its main branches and pancreatic arteries

| Artery | ND-CM[§] | LD-CM[§] | VMI+ LD-CM[§] | $p_1$ value[†] | $p_2$ value[†] | $p_3$ value[†] |
|---|---|---|---|---|---|---|
| Aorta | 4 (4,4) | 4 (4,4) | 4 (4,4) | 0.0012 | 0.5033 | 0.0087 |
| Celiac artery | 4 (4,4) | 4 (4,4) | 4 (4,4) | 0.0012 | 0.5033 | 0.0087 |
| SMA | 4 (4,4) | 4 (4,4) | 4 (4,4) | 0.0012 | 0.5033 | 0.0087 |
| PSPDA* | 2 (1,2) | 1 (1,2) | 2 (1,2) | 0.0040 | 0.5982 | 0.0172 |
| ASPDA* | 2 (2,2) | 2 (1,2) | 2 (1.5,2) | < 0.0001 | 0.0799 | 0.0033 |
| IPDA* | 3 (0,3) | 2 (0,3) | 2 (0,3) | 0.0039 | 0.0929 | 0.2059 |
| AIPDA* | 2 (1,2) | 1 (0,2) | 2 (0,2) | 0.0003 | 0.7509 | 0.0008 |
| PIPDA* | 2 (1,2) | 1 (1,2) | 2 (1,2) | 0.0005 | 0.3691 | 0.0082 |
| DPA* | 2 (2,3) | 2 (1,3) | 2 (1,3) | 0.0040 | 0.1918 | 0.1038 |
| TPA* | 2 (1,3) | 2 (0,2) | 2 (0,3) | 0.0016 | 0.9163 | 0.0012 |
| GPA* | 2 (1,3) | 1 (1,2) | 2 (1,3) | 0.0008 | 0.9275 | 0.0011 |
| CPA* | 1 (0,2) | 1 (0,2) | 1 (0,2) | 0.0002 | 0.1016 | 0.0230 |

Data are means ± standard deviations or Median (P25, P75)

**PSPDA* posterior superior pancreaticoduodenal artery, *ASPDA* anterior superior pancreaticoduodenal artery, *IPDA* inferior pancreaticoduodenal artery, *AIPDA* anterior inferior pancreaticoduodenal artery, *PIPDA* posterior inferior pancreaticoduodenal artery, *DPA* dorsal pancreatic artery, *TPA* transverse pancreatic artery, *GPA* great pancreatic artery, *CPA* caudal pancreatic artery

[§] *ND-CM* normal dose contrast medium (320 mgI/kg), *LD-CM* low dose contrast medium (224 mgI/kg), *VMI+ LD-CM images* advanced virtual monoenergetic imaging of LD-CM images

[†] $P_1$: the difference between ND-CM images and LD-CM images; $P_2$: the difference between ND-CM images and VMI+ LD-CM images; $P_3$: the difference between LD-CM images and VMI+ LD-CM images by using the Friedman test. $p < 0.05$ is considered statistically significant

The visualization of the abdominal artery, celiac artery, SMA were graded using a 4-point scale: 1 = no depiction, 2 = faint depiction, 3 = good depiction and 4 = excellent depiction. The depiction of pancreatic arteries was graded using a 4-point scale: 0 = not visible, 1 = partially visible, 2 = partially invisible or slightly irregular appearance, 3 = completely visible

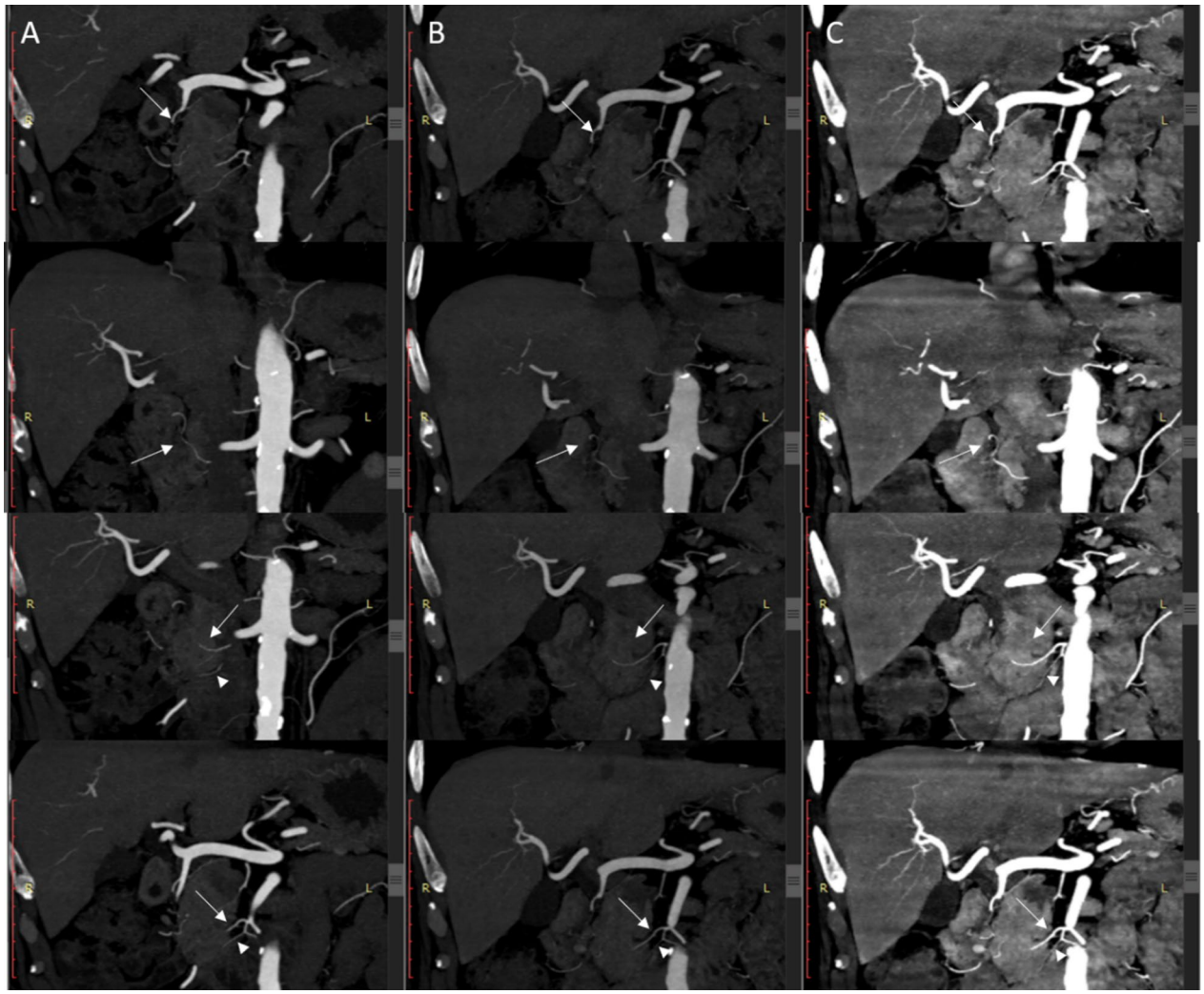


**Fig. 2** Depiction of pancreatic arteries in ND-CM, LD-CM, and VMI+ LD-CM images. **a**–**c** The posterior pancreaticoduodenal artery arch of one patient who underwent ND-CM (0.8 mL/kg, 400 mgI/mL, and 320 mgI/kg), LD-CM (0.56 mL/kg, 400 mgI/mL, and 224 mgI/kg), and VMI+ LD-CM using the same window level (300 HU) and width (600 HU). The CT value of the aorta was highest on VMI+ LD-CM images (**c**), lower on ND-CM images (**a**), and lowest on LD-CM images (**b**). The posterior pancreaticoduodenal artery arch (white arrow) can be depicted clearly on all images. The anterior inferior pancreaticoduodenal artery (AIPDA) (arrowhead) on LD-CM images (**b**) cannot be seen clearly, which showed a faint display on VMI+ LD-CM images (**c**) and can be seen clearly on ND-CM images (**a**). *ND-CM* normal-dose contrast medium, *LD-CM* low-dose contrast medium, *VMI+* advanced virtual monoenergetic imaging

## Discussion

Our study demonstrated that on the condition of constant IDR, reduced iodine dose could affect the depiction of both large-vessels and pancreatic arteries. However, the VMI+ could reduce the impact. By using the combination of VMI+ and high-concentration CM (400 mgI/mL), ultra-low-dose (224 mgI/kg) CM could be used for the depiction of both large vessels

(See figure on next page.)

**Fig. 3** Histograms of the subjective scores of artery depiction in ND-CM, LD-CM, and VMI+ LD-CM images. Histograms show the subjective scores of the abdominal aorta, its main branches, and pancreatic arteries in ND-CM (0.8 mL/kg, 400 mgI/mL, and 320 mgI/kg), LD-CM (0.56 mL/kg, 400 mgI/mL, and 224 mgI/kg), and VMI+ LD-CM images. Visualization of the abdominal artery, celiac artery, and superior mesenteric artery (SMA) were graded using a 4-point scale: 1 = no depiction, 2 = faint depiction, 3 = good depiction, and 4 = excellent depiction. The depiction of pancreatic arteries was graded using a 4-point scale: 0 = not visible, 1 = partially visible, 2 = partially invisible or slightly irregular appearance, and 3 = completely visible. *ND-CM* normal-dose contrast medium, *LD-CM* low-dose contrast medium, *VMI+* advanced virtual monoenergetic imaging

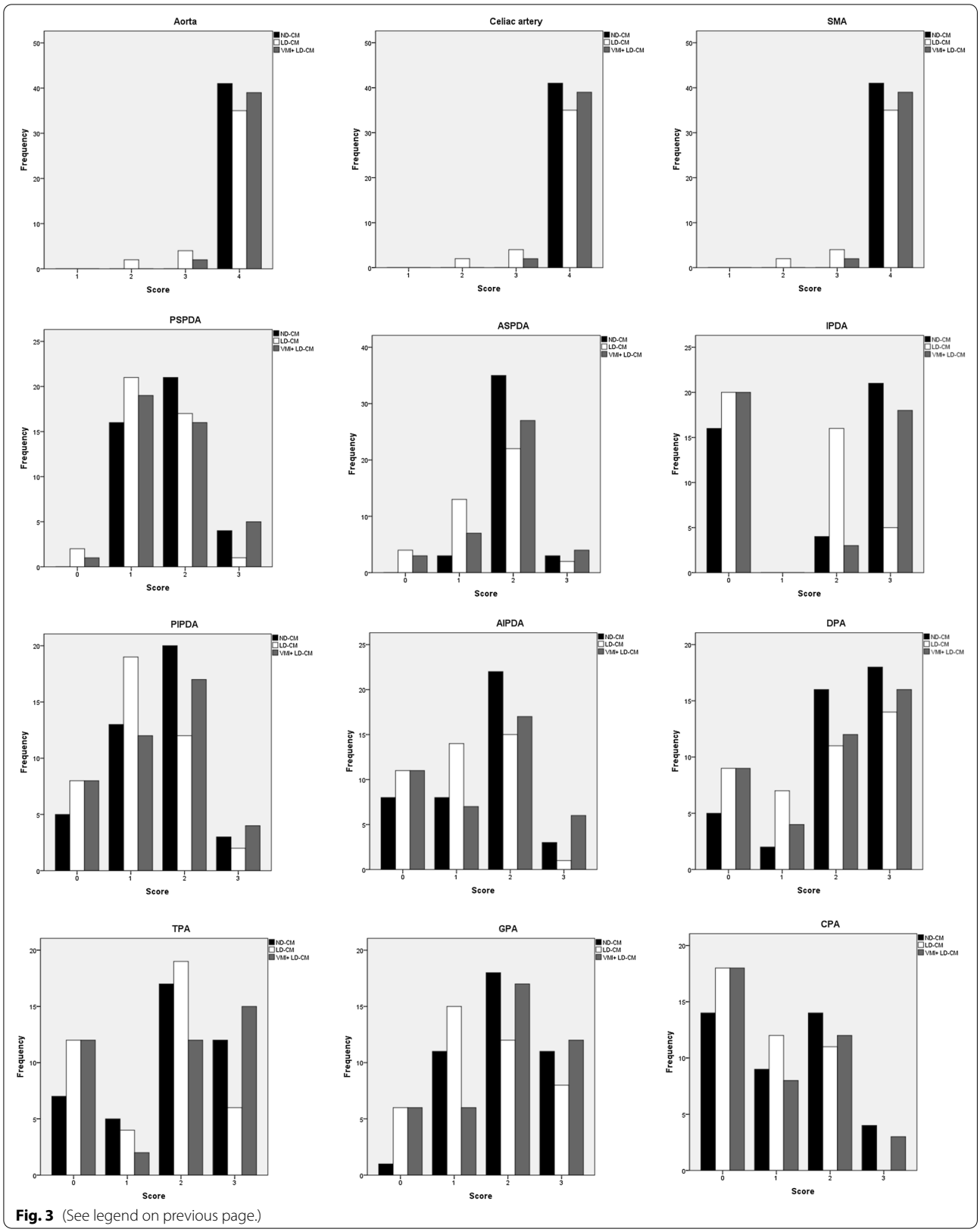


**Fig. 3** (See legend on previous page.)

and pancreatic arteries in abdominal CTA without losing the image quality compared to the normal dose (320 mgI/kg). The amount of contrast agent in the ND-CM group is 52.6 ± 9.4 mL, which exceeds the volume of a CM bottle of 50 mL, whereas the volume used in the LD-CM group was less than 50 mL (37.0 ± 6.7 mL). This imaging strategy may reduce the CM dosage and save half of CM costs, especially for patients requiring follow-up by CTA.

The dose of CM in our ND-CM group (320 mgI/kg) was lower than that in the previously reported ND-CM group (600 mgI/kg) [6, 15]. Despite this, the depiction rate of pancreatic arteries in this study was comparable to that reported previously [4, 7]. Notably, the depiction rate for IPDA (60.98%) corroborated with the findings of another study [21], in which 65% of the population had inferior origins of both the anterior and posterior arcades, leaving the SMA as a short common trunk. The difference in the depiction rates of GPA and CPA between Macchi V's study [7] and our study (73.1% and 96.2% vs. 97.56% and 65.85%, respectively) may be attributed to the different definitions of these arteries. In our study, if multiple arteries arose from the mid-to-distal one-third portion of the splenic artery, the largest one was considered the GPA, but if only one artery was depicted, the location of the artery was used to determine whether it was the GPA or CPA (the artery near the splenic hilum was considered the CPA, and that near the pancreatic body was considered the GPA). To our knowledge, the CM dose used in our study is the lowest dose used for small abdominal arteries; therefore, we called the CM dose of the LD-CM group ultra-low-dose.

The ND-CM (320 mgI/kg) images are quantitatively and qualitatively better than the LD-CM (224 mgI/kg) images, likely due to the following two factors: first, the reduced CM volume leads to reduced enhancement magnitude; second, the reduced injection time results in a narrow peak of vascular enhancement [22], which may be missed in some patients. In our study, although the depiction of pancreatic arteries in four patients was good in the ND-CM images, it was almost invisible in the LD-CM or VMI+ LD-CM images because the enhancement degree of the portal venous system was close to or exceeded that of the proximal artery. The qualitative scores of all arteries in the VMI+ LD-CM group were comparable to those of the ND-CM group (all $p > 0.05$), whereas the depiction rates of some pancreatic arteries in the VMI+ LD-CM images were lower than those in ND-CM images, which implies that VMI+ could improve the visualization of arteries only when they can be depicted on LD-CM images. In addition, this also suggests that the strategy of bolus tracking to capture the accurate time-to-peak of the aorta might not be precise for all patients. Patient-specific individualized trigger-delay technique [23] may be needed to reduce CM in abdominal CTA [13].

The VMI+ technique has been used in CTA of the head and neck [24], aorta [25], thorax, abdomen [26], and lower extremities [27, 28]. Most of these studies focused on improving the image quality. To the best of our knowledge, this technique has not been used as a compensation strategy for the possible inferior image quality of small arteries, such as pancreatic arteries, in CT angiography resulting from low iodine dose. Our results demonstrate that using VMI+ and high-concentration CM (400 mgI/kg), the CM dose could be reduced up to 70% of the ND-CM in the depiction of pancreatic arteries; this finding is in accordance with the findings of a previous study conducted by Holalkere NS et al. [15], which showed that using high-concentration CM (370 mgI/mL), the third to fifth order branches of SMA could be depicted clearly with a 20% less iodine dose. On the other hand, Sugawara H et al. found that VMI failed to provide clear visualization of small arteries by comparing full-iodine-dose (600 mgI/kg) conventional CT and half-iodine-dose (300 mgI/kg) VMI for the depiction of abdominal arteries. Although the depiction of large vessel was comparable between the full-iodine-dose conventional CT and half-iodine-dose VMI [6]. The reasons for this contradiction may be the following: (1) the CM dose reduction in their study is more than that in our study (50% vs. 30%); (2) the CM concentration in their study was less than that in our study (300 mgI/kg vs. 400 mgI/kg); (3) the injection protocol in their study was constant injection duration, whereas that in our study was constant injection rate; thus, reasons 2 and 3 caused different IDRs between their and our studies; (4) the different techniques and energy levels chosen for post-processing (VMI of 52 keV in their study vs. VMI+ of 40 keV in our study). Further, Albrecht MH et al.'s study [26] reported that image contrast and visualization of small artery branches in VMI+ images at the energy level of 40–50 keV are superior to traditional VMI images.

Our study has some limitations: first, some patients with progressive disease or partial response disease were not excluded, and there may be a difference in the artery conditions between the first examination and the follow-up due to different disease conditions. However, we tried to minimize the effect by randomizing the examination sequence and found that the artery depiction was comparable between the first examination and follow-up in these patients; second, the same injection rate rather than the same injection duration was used for ND-CM and LD-CM groups, making it difficult to capture the time-to-peak of the aorta. Therefore, an injection protocol using the same injection duration or

scanning protocol for individual-delay bolus tracking may be applied in a future study. Finally, we did not further group the patients according to body mass index (BMI) to assess whether the protocol could be used in patients with high BMI, which may be addressed in the future.

In conclusion, using the combination of VMI+ and high-concentration CM (400 mgI/mL), ultra-low-dose CM (224 mgI/kg) could be used for the depiction of both large vessels and pancreatic arteries in abdominal CTA.

#### Abbreviations

AIPDA: Anterior inferior pancreaticoduodenal artery; ASPDA: Anterior superior pancreaticoduodenal artery; BMI: Body mass index; CM: Contrast medium; CNR: Contrast-to-noise ratio; CPA: Caudal pancreatic artery; DPA: Dorsal pancreatic artery; GPA: Great pancreatic artery; IDR: Iodine delivery rate; IPDA: Inferior pancreaticoduodenal artery; LD-CM: Low dose CM; MIP: Maximum intensity projection; ND-CM: Normal dose CM; PIPDA: Posterior inferior pancreaticoduodenal artery; PSPDA: Posterior superior pancreaticoduodenal artery; ROI: Regions of interest; SD: Standard deviation; SMA: Superior mesenteric artery; SNR: Signal-to-noise ratio; TPA: Transverse pancreatic artery; VMI: Virtual monochromatic imaging; VMI+: Advanced virtual monoenergetic imaging.

#### Authors' contributions

Study Concepts: FLZ, QX, HDX, ZYJ. Data Acquisition: YHW, FLZ, HDX. Statistical Analysis: JL, CRZ. Manuscript Preparation: JL. Manuscript Editing and Reviewing: XYC, YL, YFW, HDX. All authors read and approved the final manuscript.

#### Funding

Funding was provided by National Key Research and Development Program of China (Grant No. 2020YFC2002702) and Sky imaging research fund of Chinese International Medical Foundation (Grant No. z-2014-07-1912-08).

#### Availability of data and materials

The datasets used and/or analyzed during the current study are available from the corresponding authors on reasonable request.

## Declarations

#### Ethics approval and consent to participate

This prospective study was approved by the Institutional Review Board of Peking Union Medical College Hospital. Written informed consent was obtained from all patients.

#### Consent for publication

Not applicable.

#### Competing interests

Author Xin-yue Chen is an employee of Siemens Healthineers and authors Yun Lin and Yi-fan Wu are employees of Bracco Imaging. The remaining authors declare no relationships with any companies whose products or services may be related to the subject matter of the article.

#### Author details

[1]Department of Radiology, State Key Laboratory of Complex Severe and Rare Disease, Peking Union Medical College Hospital, Chinese Academy of Medical Sciences, Peking Union Medical College, Beijing, China. [2]CT Collaboration, Siemens-Healthineers, China. [3]Global Medical and Regulatory Affairs, Bracco Imaging Medical Technologies Co., Ltd, Shanghai, China. [4]Department of Epidemiology and Health Statistics, West China School of Public Health and West China Fourth Hospital, Sichuan University, Chengdu, China. [5]Department of General Surgery, Peking Union Medical College Hospital, Chinese Academy of Medical Sciences, Peking Union Medical College, Beijing, China.

Received: 1 March 2021 Accepted: 18 July 2021
Published online: 12 November 2021

#### References

1. Hansen NJ (2016) Computed tomographic angiography of the abdominal aorta. Radiol Clin N Am 54:35–54
2. Al-Hawary MM, Francis IR, Chari ST et al (2014) Pancreatic ductal adenocarcinoma radiology reporting template: consensus statement of the Society of Abdominal Radiology and the American Pancreatic Association. Radiology 270:248–260
3. Bush WH, Swanson DP (1991) Acute reactions to intravascular contrast media: types, risk factors, recognition, and specific treatment. AJR Am J Roentgenol 157:1153–1161
4. Ishigaki S, Itoh S, Satake H, Ota T, Ishigaki T (2007) CT depiction of small arteries in the pancreatic head: assessment using coronal reformatted images with 16-channel multislice CT. Abdom Imaging 32:215–223
5. ESUR Guidelines on Contrast Agents 10.0. http://www.esur.org/esur-guidelines/. Accessed 9 Dec 2019
6. Sugawara H, Suzuki S, Katada Y et al (2019) Comparison of full-iodine conventional CT and half-iodine virtual monochromatic imaging: advantages and disadvantages. Eur Radiol 29:1400–1407
7. Macchi V, Picardi EEE, Porzionato A et al (2017) Anatomo-radiological patterns of pancreatic vascularization, with surgical implications: clinical and anatomical study. Clin Anat 30:614–624
8. Ishizaki Y, Sugo H, Yoshimoto J, Imamura H, Kawasaki S (2010) Pancreatoduodenectomy with or without early ligation of the inferior pancreatoduodenal artery: comparison of intraoperative blood loss and short-term outcome. World J Surg 34:2939–2944
9. Covantev S, Mazuruc N, Belic O (2019) The arterial supply of the distal part of the pancreas. Surg Res Pract 2019:5804047
10. Nijhof WH, van der Vos CS, Anninga B, Jager GJ, Rutten MJ (2013) Reduction of contrast medium volume in abdominal aorta CTA: multiphasic injection technique versus a test bolus volume. Eur J Radiol 82:1373–1378
11. Nijhof WH, Baltussen EJ, Kant IM, Jager GJ, Slump CH, Rutten MJ (2016) Low-dose CT angiography of the abdominal aorta and reduced contrast medium volume: assessment of image quality and radiation dose. Clin Radiol 71:64–73
12. Seehofnerova A, Kok M, Mihl C et al (2015) Feasibility of low contrast media volume in CT angiography of the aorta. Eur J Radiol Open 2:58–65
13. Gutjahr R, Fletcher JG, Lee YS et al (2019) Individualized delay for abdominal computed tomography angiography bolus-tracking based on sequential monitoring: increased aortic contrast permits decreased injection rate and lower iodine dose. J Comput Assist Tomogr 43:612–618
14. Nijhof WH, van der Vos CS, Anninga B, Stegehuis PL, Jager GJ, Rutten MJ (2013) Reduced contrast medium in abdominal aorta CTA using a multiphasic injection technique. Eur J Radiol 82:252–257
15. Holalkere NS, Matthes K, Kalva SP, Brugge WR, Sahani DV (2011) 64-Slice multidetector row CT angiography of the abdomen: comparison of low versus high concentration iodinated contrast media in a porcine model. Br J Radiol 84:221–228
16. Grant KL, Flohr TG, Krauss B, Sedlmair M, Thomas C, Schmidt B (2014) Assessment of an advanced image-based technique to calculate virtual monoenergetic computed tomographic images from a dual-energy examination to improve contrast-to-noise ratio in examinations using iodinated contrast media. Invest Radiol 49:586–592
17. Kanematsu M, Goshima S, Kawai N et al (2015) Low-iodine-load and low-tube-voltage CT angiographic imaging of the kidney by using bolus tracking with saline flushing. Radiology 275:832–840
18. Shuman WP, Chan KT, Busey JM, Mitsumori LM, Koprowicz KM (2016) Dual-energy CT aortography with 50% reduced iodine dose versus single-energy CT aortography with standard iodine dose. Acad Radiol 23:611–618
19. Mileto A, Ramirez-Giraldo JC, Marin D et al (2014) Nonlinear image blending for dual-energy MDCT of the abdomen: can image quality be preserved if the contrast medium dose is reduced? AJR Am J Roentgenol 203:838–845
20. Macchi V, Tiengo C, Porzionato A et al (2014) Anatomical remodelling of the anterior abdominal wall arteries in obesity. Clin Hemorheol Microcirc 57:255–265

21. Wacker F, Lippert H, Pabst R (2018) Arterial variations in humans: key reference for radiologists and surgeons (classification and frequency)||18 Pancreatic arteries. https://doi.org/10.1055/b-0038-149876
22. Bae KT (2010) Intravenous contrast medium administration and scan timing at CT: considerations and approaches. Radiology 256:32–61
23. Hinzpeter R, Eberhard M, Gutjahr R et al (2019) CT Angiography of the aorta: contrast timing by using a fixed versus a patient-specific trigger delay. Radiology 291:531–538
24. Leithner D, Mahmoudi S, Wichmann JL et al (2018) Evaluation of virtual monoenergetic imaging algorithms for dual-energy carotid and intracerebral CT angiography: effects on image quality, artefacts and diagnostic performance for the detection of stenosis. Eur J Radiol 99:111–117
25. Martin SS, Wichmann JL, Weyer H et al (2017) Endoleaks after endovascular aortic aneurysm repair: improved detection with noise-optimized virtual monoenergetic dual-energy CT. Eur J Radiol 94:125–132
26. Albrecht MH, Trommer J, Wichmann JL et al (2016) Comprehensive comparison of virtual monoenergetic and linearly blended reconstruction techniques in third-generation dual-source dual-energy computed tomography angiography of the thorax and abdomen. Invest Radiol 51:582–590
27. Wichmann JL, Gillott MR, De Cecco CN et al (2016) Dual-energy computed tomography angiography of the lower extremity runoff impact of noise-optimized virtual monochromatic imaging on image quality and diagnostic accuracy. Invest Radiol 51:139–146
28. Mangold S, De Cecco CN, Schoepf UJ et al (2016) A noise-optimized virtual monochromatic reconstruction algorithm improves stent visualization and diagnostic accuracy for detection of in-stent re-stenosis in lower extremity run-off CT angiography. Eur Radiol 26:4380–4389


## Publisher's Note